

## New type intraband quantum well laser

V. Ya. Aleshkin, A. A. Andronov and E. V. Demidov

Institute for Physics of Microstructures, RAS, 603600 N. Novgorod, GSP-105, Russia

**Abstract.** A universal intraband IR laser scheme on  $\Gamma-\Gamma$  and  $X-\Gamma$  valley transitions in GaAs-AlAs-like MQW systems under hot electron transfer from  $\Gamma$  valley in GaAs to  $X$  valleys in AlAs in a high lateral electric field is proposed, evaluated and simulated by the Monte-Carlo method. For a GaAs-AlAs MQW structure discussed the lasing electric field thresholds were found to be 8 kV/cm and 14 kV/cm with amplification coefficient of  $300\text{ cm}^{-1}$  and  $50\text{ cm}^{-1}$  near the thresholds at 80 K and 300 K at wavelength  $\lambda \approx 9\text{ }\mu\text{m}$ .

### Introduction

For a number of applications there is a need to have a semiconductor source working in the wavelength band from far to mid IR. Existing and emerging semiconductor lasers of the sort: intraband semiconductor lasers — i.e., p-Ge hot hole FIR lasers [1], mid IR quantum cascade lasers [2] and quantum fountain laser [3] for a number of reasons do not meet many of the application needs. So a search for the new sources is still under way.

In this work we propose a new simple universal intraband laser scheme [4] based on hot electron phenomena in GaAs-AlAs-like MQW structures under lateral transport, namely, intervalley transfer (IVT) and real space transfer (RST) of electrons. Also a thorough evaluation of the laser parameters for one specific case is made. Essentially, the scheme provides IR lasing in a planar Gunn-like diode made of the MQW structure. The laser cavity can be produced e.g. by forming of an optical restriction layer between the insulating substrate and the MQW structure and by providing a waveguide on top of the MQW system between the diode contacts. The low frequency Gunn oscillations (which the considered laser systems are potentially subject to) may be suppressed by means known in the planar Gunn devices. The scheme offers diverse possibilities and is flexible; it should provide lasing at any wavelength in a broad band from far to mid IR outside the reststrahlen region of the MQW system.

### 1 Inversion scheme

The considered MQW structures are such that the lowest electronic level of the system is the GaAs  $\Gamma$ -valley level, while the lowest level in the AlAs layer is the so-called  $X_z$ -valley level and the levels of other valleys:  $X_x$  and  $X_y$  are situated higher (see Fig. 1). The  $X_z$ -valley is situated in the Brillouin zone along the [001] growth direction, has a large effective mass along this direction and its states are mixed with the  $\Gamma$ -valley states at a GaAs-AlAs interface [5, 6]. The  $X_x$  and  $X_y$  are the ones situated in the Brillouin zone along the [100] or [010] directions, have a low effective mass along the growth direction and have no direct interaction with the  $\Gamma$  valley.

Under a high lateral electric field the  $\Gamma$ -valley electrons perform  $\Gamma-L$ ,  $L-X$  and  $\Gamma-X$  IVT and finally are accumulated at the lowest  $X_{z1}$ -valley subband in AlAs layers. The accumulation is stronger than the one in bulk GaAs under the Gunn effect [7] due to a

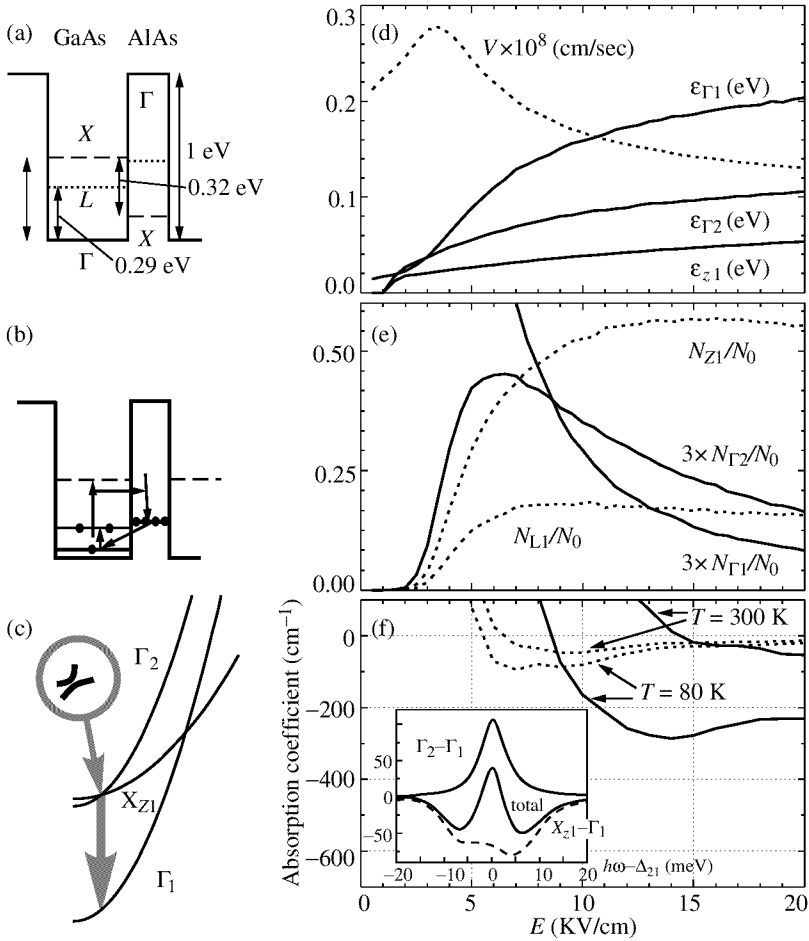


**Fig. 1.** Conduction band diagram of a single period of GaAs-AlAs MQW structure with positions of  $\Gamma$ , L and X valleys shown (a); schemes of the processes providing electron accumulation in X-valleys of AlAs,  $\Gamma_2 - \Gamma_1$  and  $X_z - \Gamma_1$  inversion and related optical transitions (b);  $\Gamma_1$ ,  $\Gamma_2$  and  $X_{z1}$  subbands versus in-plane momentum  $k$ ;  $\Gamma_2 - \Gamma_1$  and  $X_{z1} - \Gamma_1$  (hatched) laser optical transitions are indicated (c); inset shows “repulsion” of the subbands around the crossing point. Monte-Carlo simulation results at 80 K: drift velocity  $V$  and subband  $\Gamma_1$ ,  $\Gamma_2$ ,  $X_{z1}$  average kinetic energies (d); relative subband concentrations  $N_{\beta}/N_0$ ,  $N_0$  is the total electron concentration (e); peaks of absorption coefficient  $\mu$  for  $\Gamma_2 - \Gamma_1$  (solid) and  $X_{z1} - \Gamma_1$  (dash) transitions calculated from the Monte-Carlo data at  $T = 80$  K and at  $T = 300$  K and  $\chi = 1$ ; inset shows absorption coefficient spectrum at  $E = 8$  kV/cm and  $T = 80$  K (f).

substantially lower  $X_{z1}-\Gamma$  return rate through GaAs-AlAs interface. The return rate is lower due to low overlapping of the  $X_z$  and  $\Gamma$  valley wave functions. For similar reasons direct  $X_{z1}-\Gamma$  transfer due to the mixing at the interface is also rather weak. It is this accumulation [8] of electrons at the bottom of  $X_z$ -valleys that produces population inversion in the system.

Two inversions are possible here: the inversion between  $X_{z1}$  and  $\Gamma_1$  subbands and inversion between  $\Gamma_2$  and  $\Gamma_1$  subbands (see Fig. 1). The latter can arise due to preferable scattering from the  $X$ -valley subbands in AlAs to the  $\Gamma_2$  subband due to larger overlapping of the wave functions of this subband with the  $X$ -valley subbands. For the same reason a direct transfer (“injection”) of electrons to  $\Gamma_2$  subband from the lowest  $X_{z1}$  subband is also preferable. Both the inversions can be used for lasing: the radiative transition between  $\Gamma_2-\Gamma_1$  subbands has a high oscillator strength, while the  $X_z-\Gamma_1$  transition is allowed due to the wave functions admixture at the interface and is appreciable in a resonant situation when the  $\Gamma_2$  level is a little bit lower than the  $X_{z1}$  level (see Fig. 1(c)), so that there is an intersection point of these levels at some in-plane wavenumber.

As an example, we consider an AlAs/GaAs MQW structure consisting of AlAs and GaAs layers of 17 Å and 85 Å width, respectively. Conduction band diagram of a single period of the structure is given in Fig. 1(a). To describe  $\Gamma-X_z$  admixing at the interface and its effect on the  $X_z-\Gamma$  intersubband transfer rates and on the  $X_{z1}-\Gamma_1$  optical transition we use the valley intermixing potential  $H_{X_z,\Gamma} = \alpha \times \delta(z)$  [6],  $z = 0$  is the heterointerface position and  $\delta(z)$  is the delta-function. The factor  $\alpha$  estimated from the experimental data for the GaAs-AlAs interface is  $\alpha \approx 0.155$  eV cm [5]. By using the  $H_{X_z,\Gamma}$  one obtains the effective  $X_z-\Gamma$  coupling potential  $V = \alpha \psi_{X_z}(0) \psi_{\Gamma}(0)$ , where  $\psi_{X_z}(0)$ ,  $\psi_{\Gamma}(0)$  are the wave function values at the interface. For the  $\Gamma_2$  and  $X_{z1}$  subbands shown in Fig. 1(c)  $V \approx 1.4$  meV. However, at the subband crossing even small  $V$  produces “repulsion” of the subbands (shown in the inset). At the same time, electric field  $E$  is important here as well because the field produces tunneling across the gap due to the repulsion. A relative importance of the repulsion and the tunneling is determined by the ratio  $V/V_{FK}$ ,  $V_{FK} = (e^2 E^2 \hbar^2 / 2m)^{1/3}$  is the Franz–Keldish energy,  $m$  is the reduced mass:  $1/m = 1/m_{\Gamma} - 1/m_{X_z}$  where  $m_{\Gamma}$  is the effective mass in the  $\Gamma$  valley and  $m_{X_z}$  is the in-plane mass in the  $X_z$  valleys. For the electric field  $E \geq 5$  kV/cm appropriate for the inversion and lasing discussed,  $V_{FK} \geq (7-10)$  meV  $\gg V$ , and the effect of the coupling may be considered as a perturbation.

## 2 Monte-Carlo simulation results

To demonstrate the laser scheme performance we took into account intervalley scattering, polar optical phonon scattering within quantum wells via the bulk GaAs phonons and the direct  $\Gamma-X$  transitions. Results of the Monte-Carlo simulation are given in Fig. 1(d,e,f) for a lattice temperature of 80 K. One can see that electron accumulation at the  $X_{z1}$  subband starts immediately after the beginning of intervalley transfer. The condition for population inversion between  $X_{z1}$  and  $\Gamma_1$  is:  $n_{z1} > n_{\Gamma_1}$ , here  $n_{\Gamma_1}$  and  $n_{z1}$  are the occupation numbers of the  $\Gamma_1$  and  $X_{z1}$  subbands at the wave numbers corresponding to the  $\Gamma_2-X_{z1}$  subband crossing. From the simulation results it follows that the  $X_{z1}-\Gamma_1$  inversion appears at  $E > 6$  kV/cm. The condition for  $\Gamma_2-\Gamma_1$  population inversion is  $N_{\Gamma_2} > N_{\Gamma_1}$  where  $N_{\Gamma_2}$  and  $N_{\Gamma_1}$  are the surface concentrations. This inversion appears at about  $E > 8.5$  kV/cm.

The calculated peaks of the  $\Gamma_1-\Gamma_2$  and  $X_{z1}-\Gamma_1$  absorption coefficients and an example of the absorption coefficient spectrum found from the Monte-Carlo simulation results are given in Fig. 1(f). One can see that beyond the amplification thresholds the amplification coefficient is quite high ( $50 \text{ cm}^{-1}$ ) even at 300 K providing a possibility to achieve a

substantial amplification coefficient even for a low filling factor.

The considered MQW structure is the simplest example of the laser structure. In the MQW system with different layer widths (forms) and compositions one should expect a lower lasing threshold field, higher amplification coefficient and different lasing wavelength.

In particular, lasing at frequencies around transitions between the upper  $\Gamma$  subbands may be achieved. In this case a resonance between the  $X_{z1}$  subband and the upper subband of such a transition should occur (which may be achieved just by increasing the GaAs layer thickness) providing a longer lasing wavelength. On the other hand, a longer wavelength may be achieved also at the  $\Gamma_2 - \Gamma_1$  subband transition by using an appropriate  $\text{Ga}_x\text{Al}_{1-x}\text{As}$  ( $x < 0.4$ ) alloy layer instead of GaAs.

The research described in this publication was made possible due to Grants from the Russian Scientific Programs "Physics of Solid State Nanostructures" (98-02-1098), "Physics of Microwaves" (3.17), the Russian Foundation for Basic Research (99-02-17873) and the INTAS-RFBR (95-0615).

## References

- [1] *Optical and Quantum Electronics*, **23**, No 2, Special issue "FIR semiconductor lasers" (A. Andronov and E. Gornik eds.), 1991.
- [2] J. Faist, F. Capasso, D. L. Sivko, A. L. Hutchinson, and A. Y. Cho, *Science* **264**, 553 (1994).
- [3] O. Gauthier-Lafaye, P. Boucaud, F. H. Julien, S. Sauvage, S. Cabaret, J.-M. Lourtouz, V. Thierry-Mieg and R. Planel, *Appl. Phys. Lett.* **71**, 3619 (1997).
- [4] V. Ya. Aleshkin and A. A. Andronov, *JETP Lett.* **68**, 78 (1998).
- [5] J. J. Finley, R. J. Teissier, M. S. Skolnick, J. V. Cocburn, R. Grey, G. Hill and M. A. Pate, *Phys. Rev. B* **45**, R5251 (1996).
- [6] H. C. Liu, *Appl. Phys. Lett.* **51**, 1019 (1987).
- [7] M. Shur *GaAs: Devices and Circuits*, Plenum Press, 1987.
- [8] N. Z. Vagidov, Z. S. Gribnikov and V. M. Ivashenko, *Fiz. Tekh. Poluprovod.* **24**, 1087 (1990).